Bone 53 (2013) 204–215

Contents lists available at SciVerse ScienceDirect

Bone

journal homepage: www.elsevier.com/locate/bone

Original Full Length Article

Ex vivo real-time observation of Ca^{2+} signaling in living bone in response to shear stress applied on the bone surface

Yoshihito Ishihara [a,*], Yasuyo Sugawara [a], Hiroshi Kamioka [a], Noriaki Kawanabe [a], Satoru Hayano [a], Tarek A. Balam [a], Keiji Naruse [b], Takashi Yamashiro [a,*]

[a] Department of Orthodontics, Okayama University Graduate School of Medicine, Dentistry, and Pharmaceutical Sciences, Okayama, 700-8525, Japan
[b] Department of Cardiovascular Physiology, Okayama University Graduate School of Medicine, Dentistry, and Pharmaceutical Science, Okayama, 700-8558, Japan

ARTICLE INFO

Article history:
Received 22 March 2012
Revised 31 October 2012
Accepted 3 December 2012
Available online 13 December 2012

Edited by: M. Noda

Keywords:
Ex-vivo calcium imaging
Osteoblast
Osteocyte
Gap junction

ABSTRACT

Bone cells respond to mechanical stimuli by producing a variety of biological signals, and one of the earliest events is intracellular calcium ($[Ca^{2+}]_i$) mobilization. Our recently developed *ex vivo* live $[Ca^{2+}]_i$ imaging system revealed that bone cells in intact bone explants showed autonomous $[Ca^{2+}]_i$ oscillations, and osteocytes specifically modulated these oscillations through gap junctions. However, the behavior and connectivity of the $[Ca^{2+}]_i$ signaling networks in mechanotransduction have not been investigated in intact bone. We herein introduce a novel fluid-flow platform for probing cellular signaling networks in live intact bone, which allows the application of capillary-driven flow just on the bone explant surface while performing real-time fluorogenic monitoring of the $[Ca^{2+}]_i$ changes. In response to the flow, the percentage of responsive cells was increased in both osteoblasts and osteocytes, together with upregulation of *c-fos* expression in the explants. However, enhancement of the peak relative fluorescence intensity was not evident. Treatment with 18 α-GA, a reversible inhibitor of gap junction, significantly blocked the $[Ca^{2+}]_i$ responsiveness in osteocytes without exerting any major effect in osteoblasts. On the contrary, such treatment significantly decreased the flow-activated oscillatory response frequency in both osteoblasts and osteocytes. The stretch-activated membrane channel, when blocked by Gd^{3+}, is less affected in the flow-induced $[Ca^{2+}]_i$ response. These findings indicated that flow-induced mechanical stimuli accompanied the activation of the autonomous $[Ca^{2+}]_i$ oscillations in both osteoblasts and osteocytes via gap junction-mediated cell–cell communication and hemichannel. Although how the bone sense the mechanical stimuli *in vivo* still needs to be elucidated, the present study suggests that cell-cell signaling via augmented gap junction and hemichannel-mediated $[Ca^{2+}]_i$ mobilization could be involved as an early signaling event in mechanotransduction.

1. Introduction

Ca^{2+} is an important signaling messenger controlling many cellular processes, such as gene transcription, immune responses, and cell proliferation [1]. It has the ability to transduce extracellular signals (i.e., physical stress) into an intracellular response. In mammalian cells, the intracellular calcium ($[Ca^{2+}]_i$) signaling is a complex and dynamic process. One of the potentially important aspects of $[Ca^{2+}]_i$ signaling is its variety of spatial and temporal patterns and oscillatory behavior. The frequency, amplitude, and spatial localization of $[Ca^{2+}]_i$ signaling control the efficiency and specificity of many cellular responses [2–4], and such behaviors can vary depending on the cell type and different cellular functions [5,6]. Although it is generally agreed that an increase in $[Ca^{2+}]_i$ is sufficient for the stimulus–response in most excitable cells, the role of Ca^{2+} in non-excitable cells is less clear.

The biochemical signaling evoked by mechanical stress in bone cells is thought to be crucial for bone formation and remodeling via direct cell–cell communications and by soluble factors [7–9]. One of the earliest events in the bone cell mechanotransduction is $[Ca^{2+}]_i$ mobilization, which translates mechanical stimuli into biochemical signals as a messenger activating various cellular functions [10–12]. The characteristics of the $[Ca^{2+}]_i$ responses in bone cells, which are known as non-excitable cells, are modulated by their complex three-dimensional (3D) network via intercellular communications within the mineralized extracellular matrix [13–16]. These networks mainly consist of osteoblasts and osteocytes, and are thought to be able to work in synchrony to propagate locally generated signals throughout the skeletal tissue [17,18].

Previous *in vitro* studies have shown that the application of fluid shear stress to isolated osteoblasts and osteocytes results in a rapid transient increase in their $[Ca^{2+}]_i$ [13,19–21]. Although the release of Ca^{2+} and a variety of biochemical signals observed *in vitro* can very

* Corresponding authors at: 2-5-1 Shikata-cho, Kita-ku, Okayama, 700-8525, Japan. Fax: +81 86 235 6694.
E-mail addresses: ishihara@md.okayama-u.ac.jp (Y. Ishihara), yamataka@md.okayama-u.ac.jp (T. Yamashiro).

8756-3282/$ – see front matter © 2012 Elsevier Inc. All rights reserved.
http://dx.doi.org/10.1016/j.bone.2012.12.002

likely be attributed to mechanical stress, these results provide little information about the $[Ca^{2+}]_i$ signaling networks in response to mechanical stress *in vivo* or *ex vivo*, which may be a key factor revealing the bone cell mechanosensitivity. Thus, it is important to investigate the individual levels of mechanical stress-induced $[Ca^{2+}]_i$ signaling within organized tissue in order to understand how the cells in whole tissues respond to mechanical strain. To address these issues, we have recently developed a novel *ex vivo* live $[Ca^{2+}]_i$ imaging system, which makes it possible to observe the autonomous $[Ca^{2+}]_i$ oscillations. This system revealed that osteocytes specifically modulate these oscillations through gap junctions [22].

Gap junctions are thought to play an important role in the formation of the osteoblasts–osteocytes network, and are major regulators of $[Ca^{2+}]_i$ signaling [14,23–25]. Many investigators have suggested that gap junctions communicate biochemical signals evoked by mechanical stress; thus, mechanical stress may influence not only bone remodeling, but also any cellular function dependent on gap junctional intercellular communication (GJIC) [26–33]. The GJIC mediated by connexin43 (Cx43) plays an important role in the bone cell response to mechanical stimulation, and its function is probably involved in cell–cell communication. Cx43 plays essential biological roles in normal osteogenesis, craniofacial development, and in osteoblast differentiation [34]. Accordingly, Cx43 gene mutations have been linked to several debilitating diseases and tissue malformations [35]. In spite of the realization that the fluid flow activation of bone cells relies on the initiation of $[Ca^{2+}]_i$ responses [36], little is known about the regulation of GJIC in the response to the mechanical stimulation of bone cells in their natural conformation and structure, due to the relative inaccessibility of osteocytes in the mineralized matrix.

The present study clearly showed, for the first time, the dynamic elevations in $[Ca^{2+}]_i$ that occur in osteoblasts and osteocytes in the pericellular physicochemical environment. We further developed a method to apply fluid-flow stress to living bone explants in our real-time imaging system. Our experimental protocol enabled the observation of different patterns of $[Ca^{2+}]_i$ distribution between osteocytes and osteoblasts, with high temporal and spatial resolution in intact bone. To investigate the possible roles of an integrated $[Ca^{2+}]_i$ signaling network involving gap junctions among bone cells, we applied a Cx43-mediated gap junction inhibitor to this experimental system and observed the subsequent changes in $[Ca^{2+}]_i$ signaling that occurred in osteoblasts and osteocytes.

2. Materials and methods

2.1. Preparation of bone fragments

Calvariae were obtained from 16-day-old embryonic chicks and washed with alpha-modified Minimum Essential Medium (α-MEM; Invitrogen, Carlsbad, CA, USA) to remove non-adherent cells. After stripping away the periosteum, the calvariae were trimmed into 2×2 mm pieces for further use. The thickness of the samples ranged from 60 to 80 μm.

2.2. Induction of fluid flow-induced mechanical stress

Fluid flow on the capillary suction apparatus [37] was used to examine the mechano-induced $[Ca^{2+}]_i$ responses by the previously reported method [38,39], with some modifications. Bone explants were placed on glass slides (MATSUNAMI, Osaka, Japan) and held in place by a parallel-plate flow chamber using adhesive grease. Capillary diffusion-aided fluid flow was applied to the explants by adding a drop of solution to one side of the cover glass and sucking the solution from the opposite side using a piece of filter paper (Fig. 1A). We used α-MEM as flow solutions. The experiments were conducted under identical conditions; the amount of the solution, flow chamber, and the size of filter paper were all the same in each experiment. Fluorescent beads of 1.0 μm diameter (FluoSpheres (580/605), Molecular Probes) were added into the flow solution for visualization of the fluid flow. Movements of the beads were observed using a FLUOVIEW FV500 confocal laser scanning microscopy (CLS) system (Olympus, Tokyo, Japan).

2.3. Tracer labeling

Ferritin was used as a tracer material during the experiments. The chick calvariae were subjected to fluid flow stress with the vehicle (α-MEM) and ferritin tracer, and then fixed in 100% alcohol for 4 h. Visualization of the ferritin tracer was achieved by staining the end products with Perl's Prussian blue reagent, a freshly made 1:1 mixture of 4% potassium ferrocyanide and 4% hydrochloric acid (SIGMA, St. Louis, MO, USA). Calcified cross-sections (15 μm) were then cut from the blocks using a cryostat (Microm HM 500; Microm, Heidelberg, Germany) and mounted on glass slides.

2.4. Real-time reverse transcription-polymerase chain reaction (RT-PCR)

After the induction of fluid flow in the capillary suction apparatus, total RNA was isolated from the bone fragments using Isogen (Nippon Gene, Tokyo, Japan) and reverse-transcribed with the ReverTra Ace qPCR RT Kit (Toyobo, Osaka, Japan) to examine *c-fos* expression. The resulting cDNA products were subjected to a PCR analysis. PCR amplification was performed using gene-specific primers and the THUNDERBIRD SYBR qPCR Mix (Toyobo). The relative levels of the PCR products were evaluated using the LightCycler System (Roche Diagnostics, Mannheim, Germany). The gene-specific primers used for c-fos and the control 18S ribosome sequence were as follows: c-fos (accession no. M37000.1, 54 bp): sense: 5′-GAGGAGGAGAAGTCCGCTCT-3′; antisense: 5′-CTTCTCCTTCAGCAGGTTGG-3′. 18S ribosomal RNA (accession no. M59389.1, 249 bp): sense: 5′-GTTCCGACCATAAACGATGC-3′; antisense: 5′-GGAATCGAGAAAGAGCTCTCAA-3′.

2.5. Identification of bone cells

Bone cells in chick calvaria were examined three dimensionally as reported previously [40], the cells in the outer most layer were identified as osteoblasts, and the cells in the depth as osteocytes. We further examined and verified the osteoblasts on the bone surface with an alkaline phosphatase substrate, ELF-97 (enzyme-labeled fluorescence-97: Molecular Probes Inc., Eugene, OR) as described previously [13]. The explants were washed several times with PBS, and fixed with 3% paraformaldehyde in PBS for 10 min at room temperature. The samples were processed with an ELF-97 kit according to the product protocol. The identification of osteocytes in this experiment has been described in our previous publication [22].

2.6. Confocal laser scanning imaging and differential interference imaging

The osteoblasts and osteocytes in the chick calvariae were visualized with a CLS equipped for differential interference contrast (DIC) microscopy. The CLS microscopy system was coupled to an upright microscope (IX-71; Olympus) with a ×60 (NA = 1.4) oil-immersion objective lens.

2.7. Fluorescence recovery after photobleaching (FRAP) analysis

The fluid flow-induced solute transport through the bone lacunar–canalicular system was monitored using a quantitative Fluorescence Recovery After Photobleaching (FRAP) analysis [41]. Fluorescein isothiocyanate (FITC; SIGMA) was used to visualize the bone interstitial fluid space [42]. The FRAP analysis of the fluorescently-labeled lacunar–canalicular network was performed as described previously, with minor modifications [32]. In brief, bone fragments were maintained in FITC containing α-MEM at 37 °C. After recording a prebleaching image, the samples were bleached by zooming in and scanning them at maximum

laser power for 1 s. Subsequently, images were captured at the same power as was used for the pre-bleaching image. We performed the experiment within 30 min of dye loading. The FRAP data were normalized and calculated as described previously [32].

2.8. Evaluation of the viability of bone cells in intact bone explants

We used Calcein acetoxymethyl ester (Calcein-AM; Molecular Probes) to verify the cell viability and propidium iodide (PI; Molecular Probes) to detect cell death. Calcein-AM is a membrane-permeable dye that cleaved by esterases to calcein within living cells, making it a vitality marker. PI is membrane impermeable, and is excluded from live cells, making it a marker for dead cells. Calvarial bone explants were loaded with 5.0 μM Calcein-AM, 5 mg/ml PI, and 1.0 μg/ml Hoechst 33342 (Sigma) in α-MEM for 15 min at room temperature, then washed in α-MEM to remove excess dye. The explants were subsequently incubated for 45 min in α-MEM with 2% FBS at 37 °C. All viability experiments were performed 3 h after removal of the periosteum.

2.9. Calcium dye loading and imaging

The technique used to evaluate the changes in the $[Ca^{2+}]_i$ in intact bone explants has been described previously [22]. In brief, calvarial bone explants were incubated for 20 min at room temperature in α-MEM containing 10 μM fluo-8AM (ABD Bioquest, Inc., Sunnyvale, CA USA) and 10% Pluronic F-127 (ABD Bioquest, Inc.). After an additional 40 min static incubation in medium at 37 °C with humidified 5% CO_2 without dye, the bone explants were rinsed with flow medium, and coverslips were affixed to the flow chamber and mounted onto the CLS system. The scanning rate was 1.12 s/scan for 8-bit images of 512×512 pixels in size. The PMT, gain, and offset settings were the same in all experiments. Time-lapsed images were taken every 3 s, starting 15 s prior to the application of the fluid flow stress, in order to obtain the baseline intensity, until 5 min after the start of fluid flow. Fluorescence images were obtained using a krypton/argon laser at 488 nm and the light was emitted at 495 nm. The $[Ca^{2+}]_i$ was measured as the mean fluo-8 fluorescence intensity using an excitation wavelength of 488 nm. Meanwhile, we also recorded Ca^{2+} reactions for 30 min with a longer scanning interval (180 scans at 10-second intervals) to avoid any problems induced by fluorescent degradation. We used 10 μM Fura Red AM (Invitrogen), a visible light–excitable fura-2 analog, as a ratiometric Ca^{2+} imaging dye to avoid time-dependent loss of signal, as we described previously [43]. We measured the cell response of all cells in the field of view to eliminate observer bias. The fluorescence intensity of each cell just before flow treatment was used as the baseline value, and the relative increase in $[Ca^{2+}]_i$ was assessed. We defined a cell that displayed a transient increase in its $[Ca^{2+}]_i$ of at least 50% of its baseline value as a responsive cell, according to the method reported in our previous studies [13,22]. All of the responsive cells were analyzed for their peak fluorescence intensity and the cell response frequency.

2.10. Drug treatment

To evaluate the involvement of gap junctions in the responses of osteoblasts and osteocytes to fluid flow-induced mechanical stress, we pretreated the cells with 18 alpha-glycyrrhetinic acid (18 α-GA; Sigma), a reversible inhibitor of connexin43-mediated GJIC [44] and hemichannel. $GdCl_3$ (Sigma) was also used to inhibit the stretch-activated channels [45]. These drugs were dissolved in dimethyl sulfoxide (DMSO; Sigma) before being diluted in α-MEM and applied to the cells. The samples were then incubated with the drug at 37 °C under 5% CO_2 for 60 min before the experiments. The drugs were present in the medium throughout the experiment. Lastly, Ca^{2+}-free HBSS (Invitrogen) was used to replace the regular medium immediately before flow tests were performed to determine the role of extracellular Ca^{2+} [16,46]. The role of Ca^{2+} in the bone tissue was investigated using the Ca^{2+} transporting ionophore, A23187 (Sigma).

2.11. Data analysis

To compare the flow-induced changes in $[Ca^{2+}]_i$ signaling and the results of the FRAP analysis, the unpaired *t*-test or Turkey–Kramer test were used. *P* values <0.05 were considered to be significant. Significance values were calculated using a statistical analysis software program (StatView, SPSS, Chicago, IL, USA).

3. Results

3.1. Assessment of fluid flow-induced mechanical stress under our experimental conditions

We developed a fluid flow platform to measure the time course of the $[Ca^{2+}]_i$ changes that occurred in living bone explants in response to mechanical stress (Fig. 1A). Tracer labeling was performed to confirm that the mechanical stress was being applied correctly to the bone tissue. Bone fragments were subjected to fluid flow stress using medium containing ferritin particles. After exposure to fluid flow stress, Prussian blue staining was performed to examine the distribution of the fluid. Ferritin accumulation was observed within the Prussian blue stained areas of the bone surface layer (Fig. 1B). However, no ferritin staining was observed in the negative control (Fig. 1C). These results implied that the bone surface layer had been subjected to flow-induced mechanical stress.

We added small fluorescent beads to the flow solution medium to visualize the fluid flow in order to assess the continuous fluid flow during the experiment, and quantified the bead movements induced by the capillary suction. Quantification was performed by plotting all the visible beads to follow their movements during the observation period. The beads were exposed to the fluid flow stress, and almost all the observed

Fig. 1. *A schematic drawing of the experimental setup and the localization of flow-induced mechanical stress in this experimental system.* (A) A schematic representation of the flow-induced mechanical stress setup used for automated time-lapse imaging. (B) The ferritin distribution in a chick calvarial bone explant subjected to capillary fluid flow stress in this experimental system. The arrows show the ferritin distribution. (C) Chick embryonic calvariae do not generally show ferritin accumulation after Prussian blue staining. (D) Measurement of the fluid flow during the experiments. Fluorescent beads were added to visualize the fluid flow in this experimental system. (E–F) The results of the quantitative RT-PCR analysis of c-fos mRNA expression in calvarial bone cells. Chick calvarial bone cells were subjected to flow-induced mechanical stress (E) or were pretreated with the Ca^{2+} ionophore, A23187 (F). 18S served as an internal standard. Control (CONT) indicates untreated cells. The expression level of c-fos mRNA is represented on the Y-axis. The X-axis indicates the presence or absence of flow-induced mechanical stress (E) or the concentration and duration of A23187 treatment (F). The data are expressed as the means ± SE of six separate samples. The asterisks indicate significant differences (** $p<0.01$; *** $p<0.0001$). (G–H) Optically sliced images of fluorescently labeled and DIC images of osteoblasts (G) and osteocytes (H) in chick calvarial bone. ELF-97 facilitates the fluorescent tagging of cells with alkaline phosphatase activity. Images of the osteocytes were taken at 15 μm below the osteoblast layer. Bar = 20 μm. (I) Optically sliced images of FITC-labeled living osteocytes, and a DIC image of lacunae in chick calvarial bone. These images were taken from 15 μm below the osteoblast layer. Bar = 10 μm. (J) Time-lapse confocal images of photobleached osteocyte processes in a representative FRAP experiment. Serial images were taken before bleaching, immediately after bleaching, and at 30-sec intervals during fluorescence recovery. (K) The recovery of the fluorescence intensity. Unbleached cells were also monitored to use as reference cells. The data are expressed as the means ± SE. (L) Fluorescent staining images obtained to assess the osteoblast viability within chick calvariae. (left) A fluorescent image of living osteoblasts labeled with calcein in chick calvaria. (center) A fluorescent image of living osteoblasts labeled with propidium iodide (PI) in chick calvaria. (right) A merged image of the fluorescent images obtained using Hoechst 33342, calcein-AM, and PI. Bar = 20 μm.

beads showed unidirectional movements along with the flow throughout the observation period in this experimental system. The control group beads did not move a marked distance in comparison to those in the fluid flow group, and the direction of the movement, if it was detected, was random. The velocity of the fluorescent beads in the fluid flow group was significantly higher in comparison to those in the

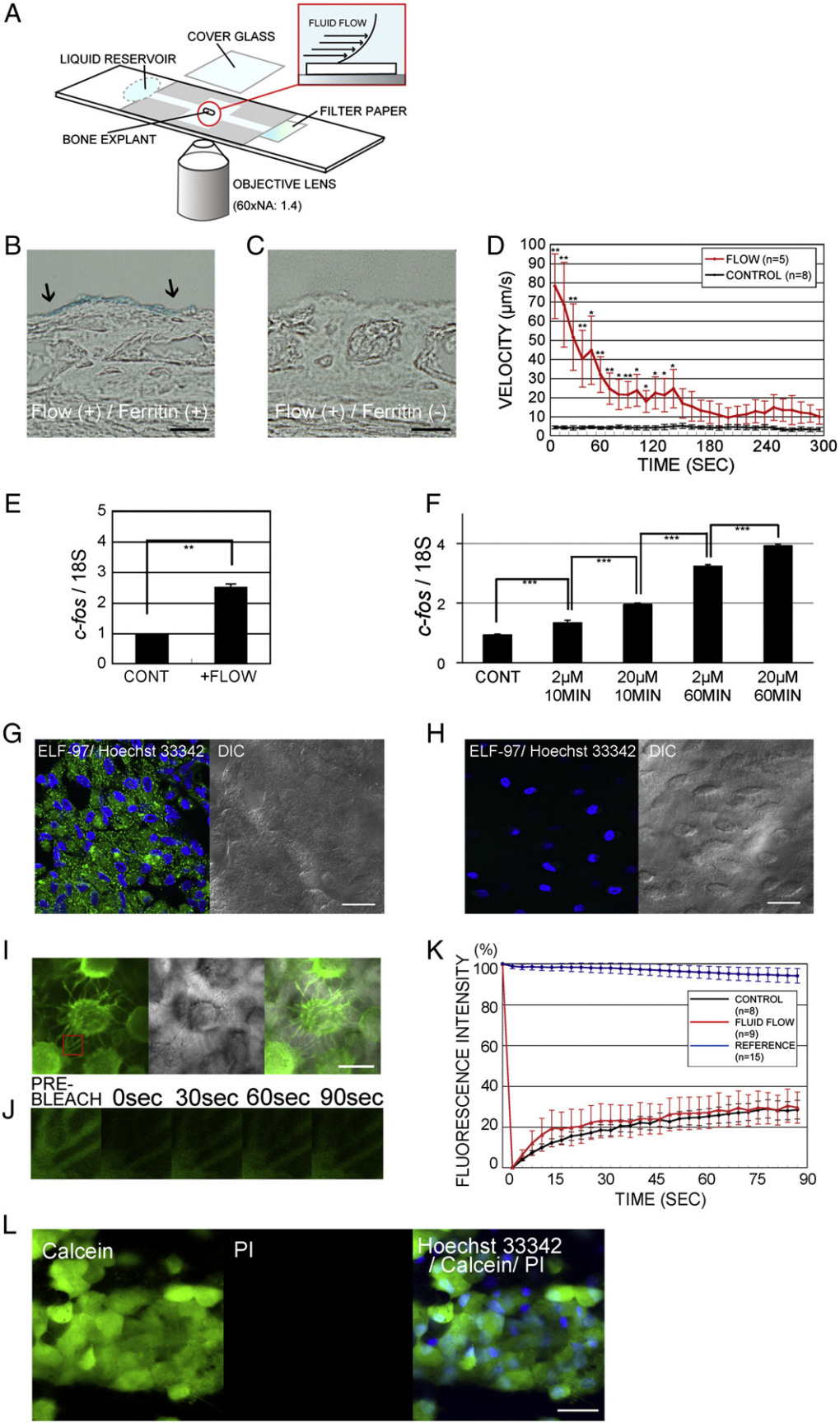

control group until 140 s (Fig. 1D; *p<0.05, **p<0.01). The fluid flow group showed higher velocity than the control group throughout the experiment even after 140 s (p<0.20 even at the least variation between two groups).

3.2. Mechano-and Ca^{2+}-induced c-fos mRNA upregulation in bone cells

We also examined whether the mechanical stress is converted into a biochemical response in this experimental system. The expression of the primary response gene, *c-fos*, was investigated in calvarial bone explants by real-time PCR. Exposure of the cells to flow-induced mechanical stress led to a rapid transient increase in *c-fos* mRNA production (Fig. 1E). The Ca^{2+}-induced expression of *c-fos* was also investigated. A23187 is an antibiotic ionophore that transports Ca^{2+} across cell membranes into the cytoplasm, and releases cations from intracellular storage sites. The Ca^{2+} ionophore dose- and time-dependently activated *c-fos* mRNA expression in the chick calvarial bone cells (Fig. 1F). These results suggested that the increases in the $[Ca^{2+}]_i$ were coupled with increases in the *c-fos* expression. Additional recordings of A23187 on the time-course of $[Ca^{2+}]_i$ level for 30 min were examined with a longer scanning interval. The results showed continuous $[Ca^{2+}]_i$ oscillation which was efficiently induced by A23187 (Supplemental Fig. 1). These $[Ca^{2+}]_i$ responses can be seen in the Supplementary Video 1.

3.3. Osteoblasts cell phenotyping in chick calvaria

The osteoblasts were identified by the detection of alkaline phosphatase activity, which is normally shown in osteoblasts but not in osteocytes, with ELF-97. The cells on the mineral-facing surface of calvaria expressed the reaction to this marker, indicating the presence of alkaline phosphate activity (Fig. 1G), whereas the activity was not detected with the cells 15 μm below the mineral-facing surface (Fig. 1H). We could sort the cells in the chick calvaria into two different populations using both DIC imaging and fluorescent imaging.

3.4. The fluid flow platform did not significantly affect the solute transport through the bone lacunar–canalicular porous areas surrounding osteocytes

In addition, we also examined the effects of mechanical stress on the deep bone layers. Several studies have suggested that the fluid flow in areas of lacunar–canalicular porosity surrounding osteocytes may be a mechanical trigger of the response to mechanical stress [47,48]. Therefore, we employed a FRAP analysis to examine the flow-induced solute transport through the bone lacunar–canalicular porous areas surrounding osteocytes. The calvarial bone lacunar–canalicular porous areas surrounding living osteocytes were stained with FITC. The staining showed osteocyte cell bodies and their processes (Fig. 1I). This technique can be used to analyze fluid flow-induced solute transport into the interstitial fluid space. In the FRAP analysis, slow recovery of fluorescence was observed due to the bidirectional transport into the photobleached canalicular tissue within 90 s of photobleaching (Fig. 1J). In the control group, the fluorescence intensity recovered to 28.4±4.6% of the prebleaching level (n=8).

Next, the intact bone explants were subjected to the same level of flow-induced mechanical stress just before the FRAP analysis. Although a higher initial fluorescence recovery rate was observed up to 30 s after photobleaching compared to the controls, the difference was not significant (n=9). The recovery of fluorescence during fluid flow had reached 29.4±7.6% after 90 s (Fig. 1K). Unbleached cells were also monitored as reference cells for photobleaching correction. The fluorescence intensity of the unbleached canalicular tissue was 94.1±3.6% after 90 s (n=15). These results indicated that mechanical stress did not affect the fluid flow in porous lacunar–canalicular tissue in this experimental model. From the histochemical staining and FRAP analysis, we confirmed that under our experimental conditions, flow-induced mechanical stress was not delivered to the osteocyte layer, but to osteoblasts residing at the bone surface.

3.5. Removal of the periosteum did not affect bone cell viability

Calvarial bone explants were loaded with the following dyes: Calcein-AM, which labels the cytoplasm of live cells; PI, which only labels the damaged cellular membranes, and Hoechst 33342, which labels nuclei. The staining pattern of individual osteoblasts and osteocytes will be described for each group below. This fluorometric assay was used in osteoblasts to evaluate whether the osteoblast layer is damaged by the removal of the periosteum. Confocal imaging clearly displayed intense green fluorescence in osteoblasts from chick calvarial explants. In contrast, red fluorescence from PI was virtually absent (Fig. 1L), indicating that the removal of the periosteum and subsequent experiments on intact bone explants did not damage the osteoblast layer.

3.6. Mechanical stress-induced $[Ca^{2+}]_i$ signaling in osteoblasts in situ

To monitor the dynamics of $[Ca^{2+}]_i$ signaling, bone cells in chick calvariae were fluorescently labeled with fluo-8AM. Fig. 2A shows a single fluo-8-loaded optical slice of the mineral-facing surface and osteoblast layer in a living bone explant. To determine the effects of mechanical stress on the $[Ca^{2+}]_i$ responses, fluid flow stress was applied to the bone explants. In most cases, the area of interest in the focal plane did not move, and images were acquired without motion artifacts. Before the initiation of flow-induced mechanical stress, we obtained five sequential X-Y images of osteoblasts present at the bone surface at 3-second intervals to provide baseline data (Fig. 2A). Fig. 2B shows the fluorescence profiles of the $[Ca^{2+}]_i$ responses observed in representative osteoblasts. Individual osteoblasts in the bone explants showed different patterns of $[Ca^{2+}]_i$ increases during the fluid-flow period. Upon the initiation of flow-induced stimulation, individual cells responded with a sudden rise in the $[Ca^{2+}]_i$, which was followed by intermittent increases in the $[Ca^{2+}]_i$ (Fig. 2B). The increased involved a rapid elevation of the $[Ca^{2+}]_i$, followed by a subsequent decline to the baseline level. Individual osteoblasts displayed oscillatory $[Ca^{2+}]_i$ increases after flow-induced mechanical stress (Fig. 2C, Video 2). The present results indicate that the $[Ca^{2+}]_i$ responses of the osteoblasts in the bone explants were increased by flow-induced mechanical stress.

3.7. Mechanical stress-induced $[Ca^{2+}]_i$ signaling in osteocytes in situ

We next changed the focal plane to obtain 2-D confocal images of the osteocytes. Fig. 3 shows confocal images of the osteocytes in intact calvarial explants. The fluorescently-labeled osteocytes could be observed 15 μm below the mineral-facing surface of the osteoblast layer (Fig. 3A). The cell bodies and their dendritic processes were fully stained. The changes in fluorescence intensity shown in Fig. 3B demonstrate the $[Ca^{2+}]_i$ oscillation in two of the representative osteocytes shown in Fig. 3A under flow-induced mechanical stress (Fig. 3B). After the initiation of flow-induced mechanical stress, individual osteocytes responded with a transient but significant increase in the $[Ca^{2+}]_i$, which was followed by further intermittent increases (arrowheads in Fig. 3C). The time courses of the $[Ca^{2+}]_i$ changes in the cells revealed that the transient increase occurred after the flow-induced mechanical stress (Figs. 3B and 3C, Video 3).

3.8. Spatio-temporal behavior of $[Ca^{2+}]_i$ responses in osteoblasts and osteocytes

Our previous *in vitro* study showed that the application of fluid flow stimulation induces changes in the $[Ca^{2+}]_i$ responses in both osteoblasts and osteocytes [13]. To clarify the effects of flow-induced mechanical stress in this *ex vivo* live Ca^{2+} imaging system, we examined the spatio-temporal patterns of the $[Ca^{2+}]_i$ response, including the percentage

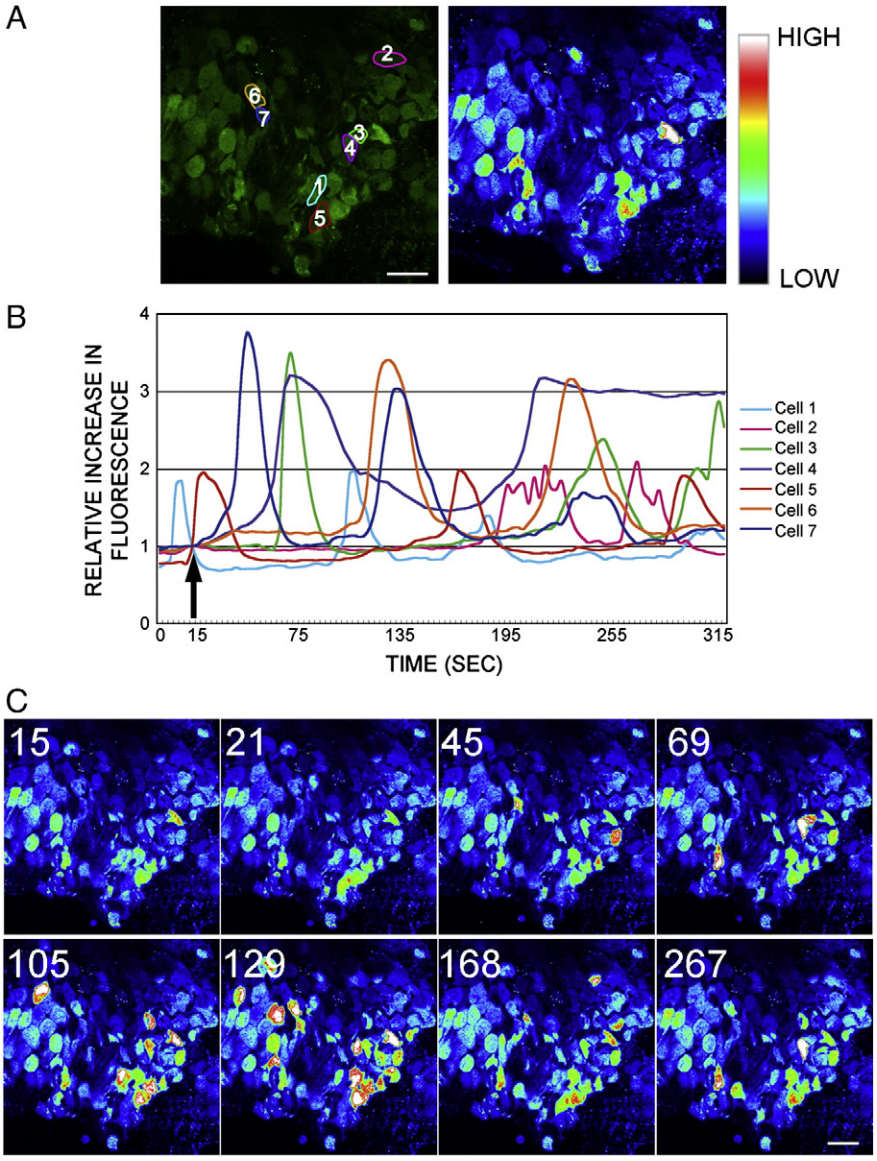

Fig. 2. *Time-lapse images of the $[Ca^{2+}]_i$ response to flow-induced mechanical stress in osteoblasts in intact calvarial explants.* (A) Fluorescent and pseudo-color images of living osteoblasts in intact calvarial explants. The color scale represents the relative fluorescence intensity. Bar = 30 μm. (B) Representative normalized relative fluorescence intensity plots of individual osteoblasts during the application of fluid flow-induced mechanical stress in intact calvarial explants. The numbers assigned to each cell indicate the cells represented in Fig. 2A, with lines of the same colors. The relative increase in fluorescence was determined by defining the mean pixel intensity observed before the flow onset as 1. The arrow indicates the initiation of flow-induced mechanical stress. Each line represents the time course of the individual $[Ca^{2+}]_i$ response of the osteoblast shown in the corresponding figure in panel A. (C) Serial pseudo-color images of the osteoblasts shown in A at 15, 21, 45, 69, 105, 129, 168, and 267 s after the initiation of monitoring. These sequential X-Y images were selected from 100 consecutive frames. Bar = 30 μm. A movie of the serial pseudo-color images can also be seen in the supplementary data (See Video 2).

of responsive cells, the peak relative fluorescence intensity, and the cell response frequency in individual osteoblasts and osteocytes (Fig. 4A). In the control group, the percentages of responsive osteoblasts and osteocytes were 14.5 ± 4.3% (n = 409 osteoblasts from 12 experiments) and 6.6 ± 1.5% (n = 403 osteocytes from 10 experiments), respectively (Fig. 4B). After the application of flow-induced mechanical stress, the percentage of responsive cells was significantly increased (46.0 ± 6.5% in osteoblasts; 16.4 ± 1.8% in osteocytes) compared to the control group in both osteoblasts ($P<0.01$) and osteocytes ($P<0.01$) (Fig. 4B).

All of the responsive cells were analyzed with regard to their peak relative fluorescence intensity and cell response frequencies. There were no significant differences between the groups in terms of the peak relative fluorescence intensity. The mean peak relative fluorescence intensity in osteoblasts with fluid flow was 2.00 ± 0.04 (n = 215 osteoblasts from 12 experiments), which was not significantly different from that in the control group (1.84 ± 0.05; n = 53 osteoblasts from 12 experiments; Fig. 4C). Similarly, the mean peak relative fluorescence intensity in osteocytes with fluid flow was 1.85 ± 0.05 (n = 36 osteocytes from 10 experiments), which was not significantly different from that in the control group (1.81 ± 0.07; n = 25 osteocytes from 10 experiments; Fig. 4C). The mean cell response frequency in osteoblasts with fluid flow was 0.32 ± 0.01/min (n = 215 osteoblasts from 12 experiments), which was significantly increased from that in the control group (0.27 ± 0.02 sec) ($p<0.05$, n = 53 osteoblasts from 12 experiments; Fig. 4D). Meanwhile, the mean cell response frequency in osteocytes with fluid flow was 0.32 ± 0.03/min (n = 36 osteocytes from 10 experiments), which was not significantly different from that in the control group (0.32 ± 0.04/min; n = 25 osteocytes from 10 experiments).

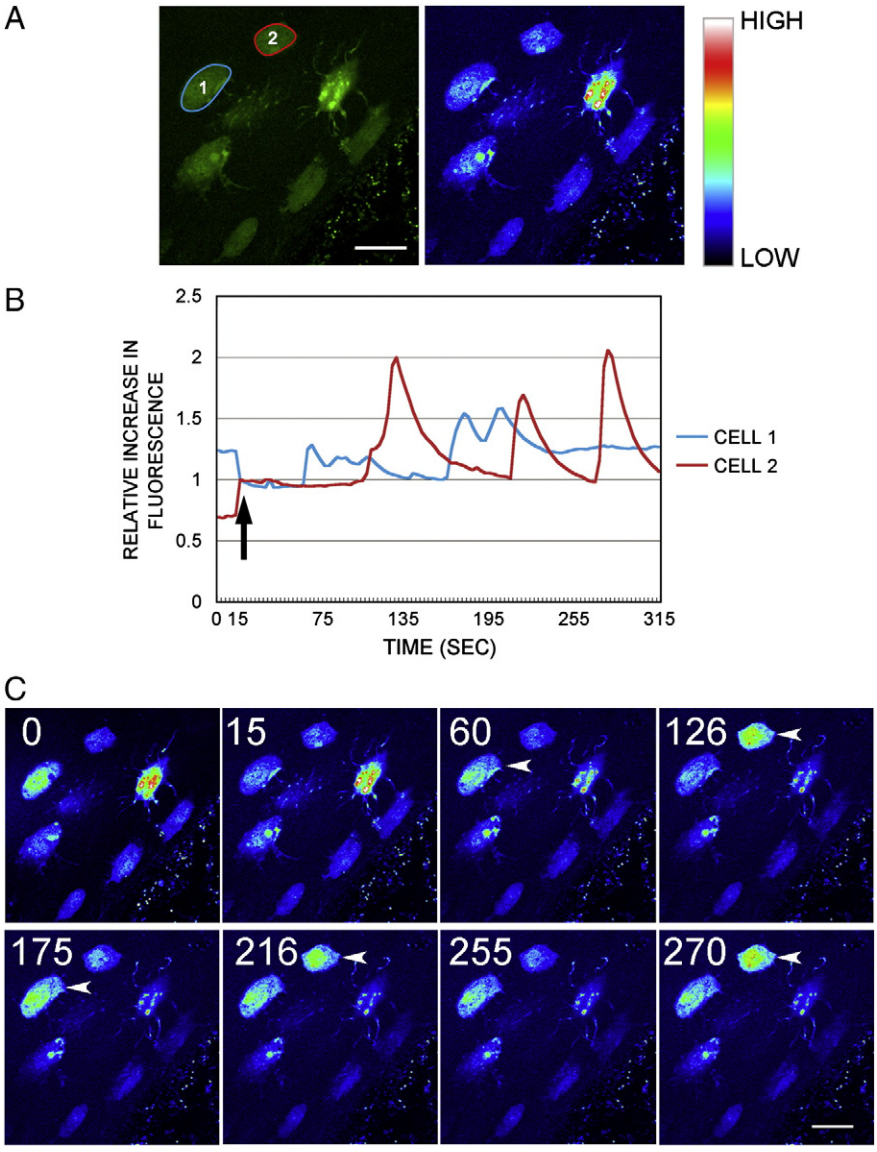

Fig. 3. *Time-lapse images of the $[Ca^{2+}]_i$ response to flow-induced mechanical stress in osteocytes in intact calvarial explants.* (A) Fluorescent and pseudo-color images of living osteocytes in intact calvarial explants. The color scale represents the relative fluorescence intensity. Bar = 10 μm. (B) Representative normalized relative fluorescence intensity plots of individual osteocytes during the application of fluid flow-induced mechanical stress in intact calvarial explants. The arrow indicates the initiation of flow-induced mechanical stress. Each line represents the time course of the individual $[Ca^{2+}]_i$ response shown by the corresponding figure in panel A. (C) Serial pseudo-color images of the osteocytes monitored in A at 0, 15, 60, 126, 175, 216, 255, and 270 s after the initiation of monitoring. The arrowheads indicate the $[Ca^{2+}]_i$ response. Bar = 10 μm. A movie of the serial pseudo-color images can also be seen in the supplementary data (See Video 3).

3.9. Blockade of gap junctions inhibits the flow-induced $[Ca^{2+}]_i$ responses in osteocytes, but this effect is minimal in osteoblasts

Osteoblasts and osteocytes form an integrated cell network, and communicate with each other via a direct cell-to-cell pathway, which is thought to be mediated by gap junctions [17,23,24,27,31,32,34,36]. We applied a gap junction inhibitor as a first step to examine whether the cellular networks contribute to maintaining these $[Ca^{2+}]_i$ responses in osteoblasts and osteocytes. Treatment with 18α-GA, a Cx43-mediated gap junction and hemichannel inhibitor, reduced the percentage of responsive osteocytes in both the control group and in the fluid flow group by 1.9 ± 0.9% ($p<0.01$) (n = 430 osteocytes from 10 experiments) and 1.7 ± 0.9% ($p<0.0001$, n = 418 osteocytes from 9 experiments), respectively (Fig. 4B). This inhibitor also caused a reduction in the mean cell response frequency of the osteocytes in the fluid flow group by 0.23 ± 0.03/min ($p<0.05$, n = 6 osteocytes from 9 experiments).

In contrast, the percentage of responsive osteoblasts was not significantly reduced by the 18α-GA treatment in either the control group or the fluid flow group (by 14.5 ± 3.7%; n = 402 osteoblasts from 10 experiments, and 32.2 ± 5.4%; n = 278 osteoblasts from 8 experiments) (Fig. 4B). The peak relative fluorescence intensity of the control groups treated with 18α-GA was 1.96 ± 0.09 in osteoblasts (n = 45 osteoblasts from 10 experiments) and 1.68 ± 0.05 in osteocytes (n = 13 osteocytes from 10 experiments). The peak relative fluorescence intensity was not affected by the 18α-GA treatment, regardless of flow-induced mechanical stress, because after treatment the values were 2.04 ± 0.07 in osteoblasts (n = 80 osteoblasts from 8 experiments) and 1.83 ± 0.18 in osteocytes (n = 6 osteocytes from 9 experiments) (Fig. 4C). Conversely, the mean cell response frequency in osteoblasts with fluid flow was significantly reduced by the 18α-GA treatment by 0.27 ± 0.01/min ($p<0.05$, n = 80 osteoblasts from 8 experiments).

We next performed the same experiments using osteocytes treated with 18α-GA to determine if the inhibitory effect of 18α-GA on the $[Ca^{2+}]_i$ signaling in osteocytes was due to chemical toxicity-related cell death. The osteocytes in calvarial explants, thus exhibiting similar results to the osteoblasts, showed a bright green fluorescence with

calcein-AM, and no red fluorescence with PI staining (Fig. 4E). Nuclear staining with Hoechst 33342 was observed in both osteoblasts and osteocytes. These results suggest that the reduced proportion of responsive osteocytes was not the result of cell death induced by 18α-GA toxicity.

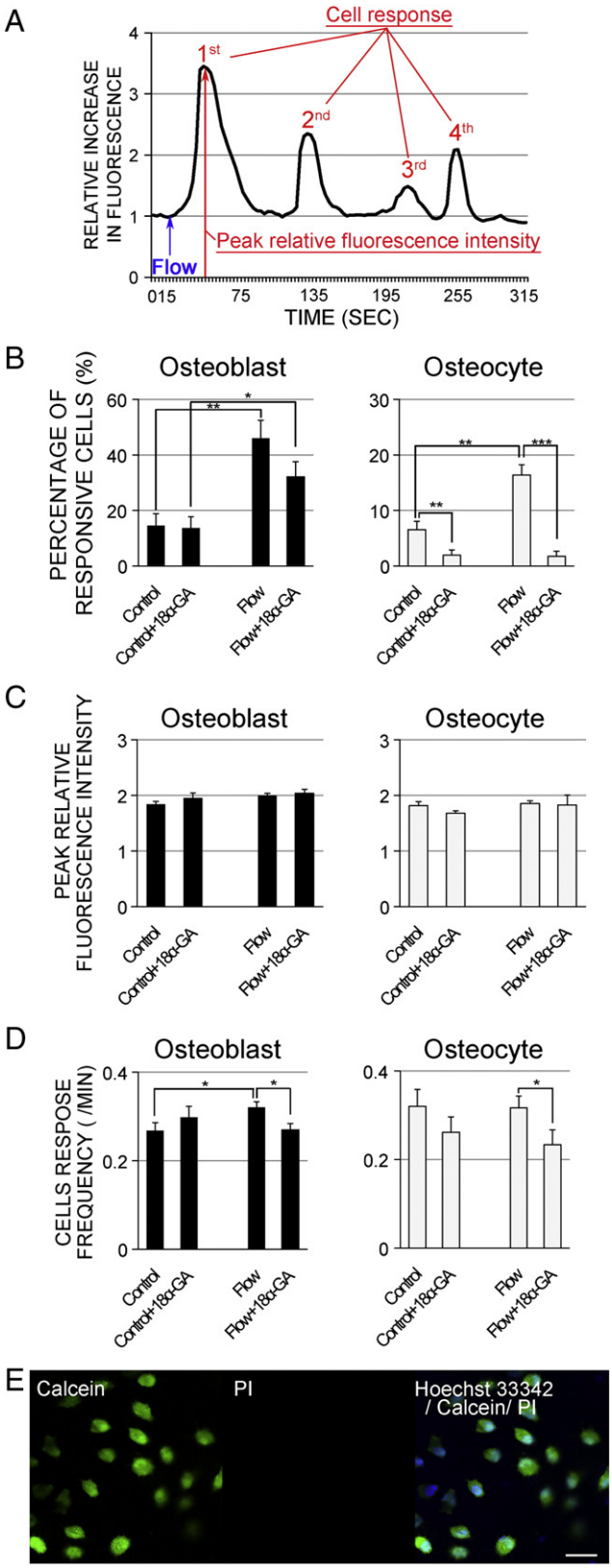

3.10. Blockade of the stretch-activated channels did not inhibit the flow-induced $[Ca^{2+}]_i$ responses in osteocytes, and this effect is minimal in osteoblasts

The effects of mechanical stress on the $[Ca^{2+}]_i$ responses were assessed in the presence of Gd^{3+}. A membrane impermeable gadolinium chloride has been reported to block the stretch-activated channels. The percentage of responsive osteoblasts was not significantly decreased by treatment with 100 μM Gd^{3+} in either the control group or the fluid flow group. (17.6 ± 4.1%; n = 324 osteoblasts from 7 experiments and 32.6 ± 7.0%; n = 324 osteoblasts from 7 experiments, respectively), (Fig. 5A), and the decrease was fairly close to the result in the 18α-GA group. The Gd^{3+} treatment group also showed an increase in the peak relative fluorescence intensity and the mean cell response frequency of the osteoblasts in the fluid flow group by 2.11 ± 0.05 (Fig. 5B) and 0.32 ± 0.02/min ($p<0.05$, n = 134 osteoblasts from 7 experiments), respectively (Fig. 5C). No decrease in the percentage of responsive cells occurred in Gd^{3+} treated osteocytes that were not close to 18α-GA treated osteocytes (Fig. 5A). The peak relative fluorescence intensity and the mean cell response frequency of the osteocytes were also not affected by the Gd^{3+} treatment, regardless of flow-induced mechanical stress (Figs. 5B and 5C).

3.11. Role of extracellular Ca^{2+} concentration in the flow-induced $[Ca^{2+}]_i$ responses in osteoblasts and osteocytes

We performed additional experiments to assess the effect of extracellular Ca^{2+} after the exposure to flow-induced mechanical stress. Ca^{2+}-free medium is observed to lower the percentage of responsive osteoblasts and osteocytes significantly under flow-induced mechanical stress (26.0 ± 6.4%; n = 402 osteoblasts from 7 experiments and 7.4 ± 5.9%; n = 216 osteocytes from 8 experiments, respectively). The addition of 18α-GA in Ca^{2+}-free medium further reduced the percentage of responsive osteoblasts and osteocytes (10.8 ± 2.7%; n = 323 osteoblasts from 7 experiments and 2.8 ± 1.8%; n = 254 osteocytes from 8 experiments, respectively), (Fig. 6A). The peak relative fluorescence intensity was not affected by the Ca^{2+}-free medium treatment, regardless of the presence of 18α-GA in both osteoblasts and osteocytes (Fig. 6B). In contrast to the results for peak relative fluorescence intensity, the application of Ca^{2+}-free medium showed a tendency to reduce the mean cell response frequency in flow-induced osteocytes (Fig. 6C).

4. Discussion

In this study, we introduced a novel approach to measure the real-time $[Ca^{2+}]_i$ dynamics in osteoblasts and osteocytes in intact calvarial explants to study the behavior and connectivity of $[Ca^{2+}]_i$ signaling networks in the mechanotransduction within living bone tissue. How bone cells sense mechanical stimuli is still largely unknown. Nevertheless, these stimuli influence cell function through cell–cell

Fig. 4. *The effect of a gap junction inhibitor on the fluid flow-induced $[Ca^{2+}]_i$ signaling observed in osteoblasts and osteocytes in intact calvarial explants.* Bone fragments were incubated in α-MEM (Control) or pretreated with 30 μM 18α-GA for 60 min before the experiments. (A) The typical $[Ca^{2+}]_i$ profile of bone cells in intact calvarial explants during the flow-induced mechanical stress. The $[Ca^{2+}]_i$ responses were recorded for 315 s: 15 s for the baseline recording and 300 s after the application of flow-induced mechanical stress. The percentage of responsive cells (B), the peak relative fluorescence intensity in the responsive cells (C), and the cell response frequency in the responsive cells (D) after the application of flow-induced mechanical stress were calculated. The data are expressed as the means ± SE. The asterisks indicate a significant difference (*$p<0.05$; ** $p<0.01$; ***$p<0.0001$). (E) Images of fluorescent staining used to assess the osteocyte viability within chick calvariae. (left) A fluorescent image of living osteocytes labeled with calcein in chick calvaria. (center) A fluorescent image of living osteocytes labeled with propidium iodide (PI) in chick calvaria. (right) A merged image of the fluorescent images obtained using Hoechst 33342, calcein-AM, and PI. Bar = 20 μm.

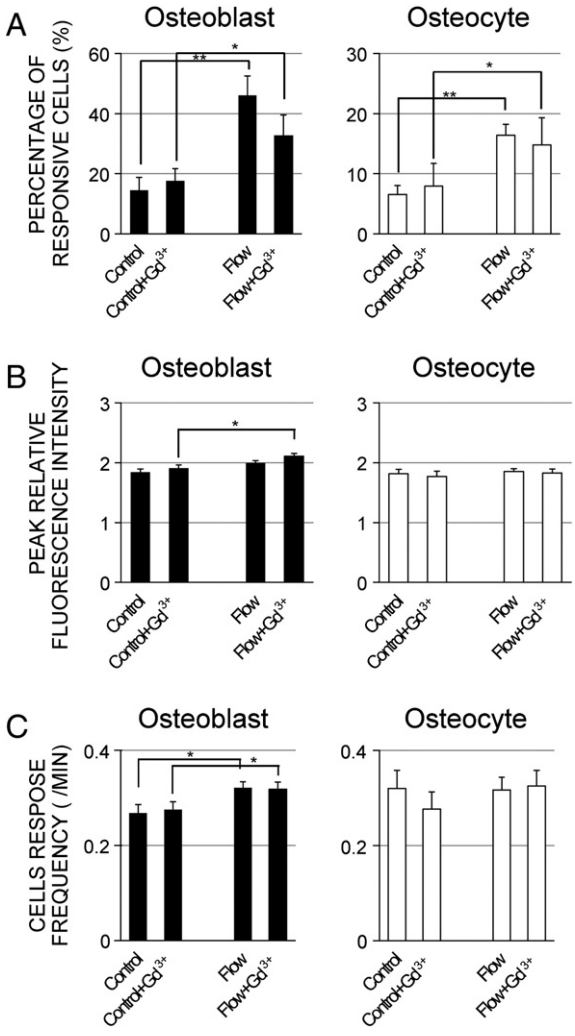

Fig. 5. *The effect of a Gd^{3+} on the fluid flow-induced $[Ca^{2+}]_i$ signaling observed in osteoblasts and osteocytes in intact calvarial explants.* Bone fragments were incubated in α-MEM (Control) or pretreated with 100 μM Gd^{3+} for 60 min before the experiments. The percentage of responsive cells (A), the peak relative fluorescence intensity in the responsive cells (B), and the cell response frequency in the responsive cells (C) after the application of flow-induced mechanical stress were calculated. The data are expressed as the means ± SE. The asterisks indicate significant difference (*$p<0.05$; ** $p<0.01$).

communication, cell–cell adhesion, or cell–matrix interactions, and it is becoming increasingly clear that mechanical stimuli collaborate with biochemical cues to modulate cell and tissue behavior. Consequently, it is desirable to use a model that closely mimics the bone microenvironment, and much better to use living bone for the analysis of cell function.

The bone is a complex tissue composed of cells, collagenous matrix, and mineral elements that provide essential functions, including mechanical support. Due to this complex morphology of bone tissue, especially of osteocytes, which are embedded in the mineralized matrix, performing multi-cellular $[Ca^{2+}]_i$ recordings within bone tissue has been difficult or impossible. Several past studies have reported the observation of an intermittent increase in $[Ca^{2+}]_i$ signaling in isolated/cultured osteoblasts and osteocytes in response to external stimuli [12–16,18,20,24]. However, the importance of this increase was unclear, because isolated osteoblasts and osteocytes cultured on a two-dimensional (2D) cell culture dish may not behave as the cells do in the complex 3D structure and microenvironment of living bone. Our novel platform is distinct from the conventional method in terms of the estimation of the $[Ca^{2+}]_i$ response at the tissue level, as well as at the level of individual cells, and provides high temporal and spatial resolution. Thus, our real-time imaging analysis provides important information regarding how osteoblasts and osteocytes convert mechanical stimuli into an early biochemical response in a more integrated environment that helps identify the physiological impact of the response.

In the present study, we examined whether the fluid flow stress was being correctly delivered to the bone surface using the fluid flow marker, ferritin. Ferritin was detected at the outer bone surface, but not inside the bone (Fig. 1B), indicating that the fluid flow stress was being delivered specifically to the bone surface. The expression of *c-fos* is rapidly and transiently induced by various mechanical stimuli including fluid shear stress [19], which may promote bone cell development [49,50]. The real-time PCR analysis demonstrated that the fluid flow-induced mechanical stress in this experimental system upregulated *c-fos* mRNA expression throughout the bone tissue (Fig. 1E). In addition, the enhancement of *c-fos* expression by mechanical stress was correlated with the $[Ca^{2+}]_i$ increase (Fig. 1F).

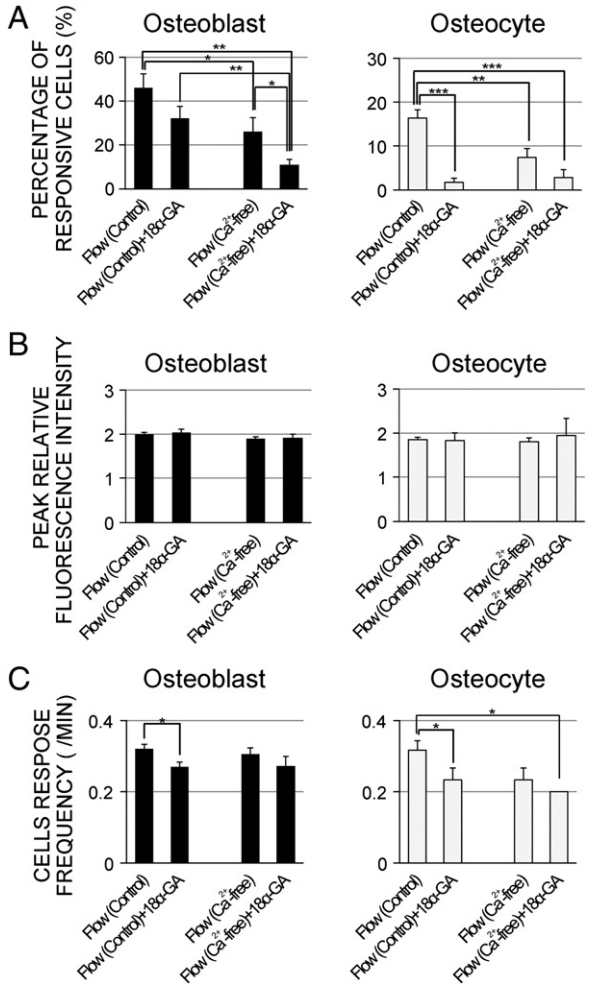

Fig. 6. *The effect of extracellular Ca^{2+} on the fluid flow-induced $[Ca^{2+}]_i$ signaling observed in osteoblasts and osteocytes in intact calvarial explants.* Chick calvarial bone cells were subjected to flow-induced mechanical stress with or without 30 μM 18α-GA. A Ca^{2+}-free solution was used to replace the regular medium immediately before the fluid flow experiments. The percentage of responsive cells (A), the peak relative fluorescence intensity in the responsive cells (B), and the cellular response frequency in the responsive cells (C) after the application of flow-induced mechanical stress were calculated. The data are expressed as the means ± SE. The asterisks indicate a significant difference (*$p<0.05$; ** $p<0.01$; ***$p<0.0001$).

The Ca^{2+} ionophore, A23187, has been extensively used to mimic the effects of many physiological cell stimuli related to Ca^{2+} [51], and the addition of the Ca^{2+} ionophore induced the upregulation of *c-fos* mRNA expression in the bone explants in this study (Fig. 1F). These results suggest that the upregulation of *c-fos* expression by flow-induced mechanical stress was linked to the $[Ca^{2+}]_i$ increases observed in this experimental system. We recorded A23187-induced $[Ca^{2+}]_i$ reactions for 30 min to examine the reasons for the increase of $[Ca^{2+}]_i$ level independent of the Ca^{2+} equilibrium potential. We clearly observed many cells repeatedly oscillating for relatively long periods of time in the presence of A23187 (Supplemental Fig. 1). These findings suggest that a higher concentration and longer A23187 treatment time further increase the *c-fos* mRNA relative expression level, and this increase is thought to be due to continuous Ca^{2+} oscillation induced by A23187. Enhanced production of *c-fos* mRNA in the incubation with A23187 has also been mentioned in the past reports with other cell types [52–54]. Schaefer and colleagues showed a rapid increase in *c-fos* mRNA within 15 min, and the expression of *c-fos* mRNA reached a maximum in 30–60 min [54]. We think that these reports strongly support our results in this experiment.

We then evaluated whether the fluid also entered the lacunar–canalicular system of the bone using a FRAP analysis (Figs. 1I and 1K). However, our FRAP analysis demonstrated that little or no liquid flow in the lacunar–canalicular system was induced by the fluid flow applied to the bone explants. The lacunar–canalicular system is essential because it serves as a continuous transport pathway connecting osteocytes with each other, as well as with osteoblasts and with the blood flow. Mechanical loading has been proposed to enhance solute transport in the lacunar–canalicular system, presumably by increasing fluid displacement [47,55–57]. It would be ideal to examine such solute transport with a protocol involving matrix deformation. Confocal microscopy is technically incapable of measuring the magnitude of stimulation induced by fluid shear stress in the lacuno-canalicular system, and this is an issue in addition to the difficulty in observing the $[Ca^{2+}]_i$ increase of bone cells *in situ* caused by matrix deformation-induced displacement of the targeted observation area. Although our experimental system does not necessarily reflect physiological conditions, it provides a suitable method for investigating how the stress-induced early cellular signals of osteoblasts located in the superficial layer of the bone are transmitted to osteocytes embedded in the bone matrix.

Our time-course $[Ca^{2+}]_i$ measurement of multiple cells *in situ* allowed us to evaluate the Ca^{2+} signaling using the following three parameters: the percentage of responsive cells, the peak relative fluorescence intensity, and the cell response frequency. Among these parameters, mechanical stress significantly increased the cell response rate by more than two-fold compared to the control value in both osteoblasts and osteocytes (Fig. 4B). The cell response frequency was also upregulated in osteoblasts by almost 20% (Fig. 4D). Conversely, no such upregulation was observed in the peak relative fluorescence intensity (Fig. 4C). These data indicate that the $[Ca^{2+}]_i$ responses are enhanced by mechanical stimuli in osteoblasts, and that such biophysical signals from the osteoblast layer are transmitted to osteocytes embedded within the bone matrix through the 3D osteoblasts–osteocytes network. In particular, the percentage of responsive cells was notably increased compared with the peak relative fluorescence intensity.

With regard to the differences between osteoblasts and osteocytes, the percentage of responding osteoblasts was higher than that of osteocytes in both the control and flow-induced mechanical stress groups (Fig. 4B). These results were in line with our previous observations regarding single primary osteoblasts and osteocytes in a 2D cell culture system [13]. In a recent study, Lu and colleagues demonstrated the $[Ca^{2+}]_i$ responses in micro-patterned *in vitro* osteocytic and osteoblastic networks [16]. They showed that osteocytic networks are more responsive than osteoblastic networks under low magnitude fluid flow stress, which was different from our results. The reason(s) for the differences in the results are unclear, and continues to be a source of controversy among researchers. We suggest that these discrepancies in flow-induced $[Ca^{2+}]_i$ signaling may be due to the differences between the *in vitro* and *ex vivo* culture systems and the absence/presence of cell–matrix interactions, lacunar-canaliculi porosity, complex morphological features, and the 3D microenvironment.

Some studies have examined the GJIC between bone cells and its role in bone cell mechanotransduction [14,16,24,26–29,36]. To further investigate the role of gap junctions in the activation of flow-induced $[Ca^{2+}]_i$ responses, the effect of 18α-GA on $[Ca^{2+}]_i$ signaling was also examined in the living bone explants. During our experiments examining the spatio-temporal patterns of the $[Ca^{2+}]_i$ response, the gap junction inhibitor 18α-GA completely inhibited the stress-induced upregulation of the percentage of responsive osteocytes (Fig. 4B). It is interesting that no such downregulation was evident in osteoblasts. These results indicated that the involvement of the GJIC and hemichannel in $[Ca^{2+}]_i$ responses differs between osteoblasts and osteocytes. On the other hand, 18α-GA pretreatment significantly decreased the cell response frequency in individual osteoblasts and osteocytes under the fluid flow conditions (Fig. 4D). It is thought that $[Ca^{2+}]_i$ signaling through frequency modulation is translated into distinct cellular responses [58]. A similar explanation was also suggested for terminally differentiated human osteoblasts [59]. Based on these results, it appears that biophysical stress may influence the cellular function in a manner that is dependent on the connexin43-mediated GJIC and hemichannel.

We have tested the involvement of stretch-activated channels in the flow-induced $[Ca^{2+}]_i$ responses. The results showed that Gd^{3+}, like 18α-GA, did not show a significant difference from control, though it decreased the osteoblastic $[Ca^{2+}]_i$ response. In contrast, Gd^{3+} did not significantly inhibit the osteocytic $[Ca^{2+}]_i$ response (Fig. 5). These data show that the stretch-activated membrane channel, blocked by Gd^{3+}, is less affected in the flow-induced $[Ca^{2+}]_i$ response. This is in contrast to the data on the steady flow where the $[Ca^{2+}]_i$ responses were inhibited by blocking this channel in osteoblasts [19]. However, our findings also suggest that our non-steady fluid flow platform induced mechanical stress in osteoblasts residing on the bone's surface (Fig. 1D), but not in the osteocytes layer (Fig. 1J). You et al. showed that Gd^{3+} did not influence the $[Ca^{2+}]_i$ responses to oscillatory fluid flow in MC3T3-E1 cells [60]. The discrepancy in these observations led to the interpretation that this fluid-flow platform does not have enough force to stimulate the Gd^{3+}-sensitive channel neither in osteoblasts nor in osteocytes.

We also confirmed the effects of Ca^{2+} from outside of the cell (with/without 18α-GA) using Ca^{2+}-free flow solution. With this additional experiment, we observed the decrease in responsive rate and response frequency both in osteoblasts and in osteocytes. This indicates that Ca^{2+} from outside of the cell has a very important role in the increase in $[Ca^{2+}]_i$ by flow-induced mechanical stress. Furthermore, this effect was reinforced by the combined use of 18α-GA. The opening of Cx43 hemichannels is infrequent in normal extracellular Ca^{2+} [61], and is enhanced under the removal of extracellular Ca^{2+} [62,63]. Although the investigation of the extracellular Ca^{2+}-free condition has been difficult due to the possible occurrence of unfavorable and unexpected influence from the lack of extracellular Ca^{2+}, it is speculated that the influence of extracellular Ca^{2+} might affect $[Ca^{2+}]_i$ via hemichannel. Therefore, our results imply that the change of this $[Ca^{2+}]_i$ level is due to the movement of Ca^{2+} via gap junctions and via Cx43 hemichannels.

In summary, we studied the real-time fluorogenic monitoring of the $[Ca^{2+}]_i$ dynamics in osteoblasts and osteocytes within intact calvarial explants. Our findings provide direct evidence that an autonomous $[Ca^{2+}]_i$ response is promoted by fluid-flow shear stress applied on the bone surface via gap junction. The results of the present study suggest that the cell–cell signaling caused by augmented gap junction and hemichannel-mediated $[Ca^{2+}]_i$ mobilization could be involved as an early signaling event in mechanotransduction.

Supplementary data to this article can be found online at http://dx.doi.org/10.1016/j.bone.2012.12.002.

Acknowledgments

The authors thank Kayo Nagasaka for many helpful comments and support in writing the manuscript. The present work was supported by a Grant-in-Aid for Scientific Research (to Y. Ishihara) from the Ministry of Education, Culture, Sports, Science and Technology, Japan as part of the Research Fellowships for Young Scientists, and was supported in part by Grants-in-Aid for Scientific Research (to T. Yamashiro) from the Japan Society for the Promotion of Science, Japan.

References

[1] Berridge MJ, Bootman MD, Lipp P. Calcium—a life and death signal. Nature 1998;395:645–8.
[2] Dolmetsch RE, Xu K, Lewis RS. Calcium oscillations increase the efficiency and specificity of gene expression. Nature 1998;392:933–6.
[3] Li W, Llopis J, Whitney M, Zlokarnik G, Tsien RY. Cell-permeant caged InsP3 ester shows that Ca^{2+} spike frequency can optimize gene expression. Nature 1998;392:936–41.
[4] De Koninck P, Schulman H. Sensitivity of CaM kinase II to the frequency of Ca^{2+} oscillations. Science 1998;279:227–30.
[5] Berridge MJ, Bootman MD, Roderick HL. Calcium signaling: dynamics, homeostasis and remodeling. Nat Rev Mol Cell Biol 2003;4:517–29.
[6] Fewtrell C. Ca^{2+} oscillations in non-excitable cells. Annu Rev Physiol 1993;55:427–54.
[7] Reich KM, Gay CV, Frangos JA. Fluid shear stress as a mediator of osteoblast cyclic adenosine monophosphate production. J Cell Physiol 1990;143:100–4.
[8] Heino TJ, Hentunen TA, Väänänen HK. Osteocytes inhibit osteoclastic bone resorption through transforming growth factor-beta: enhancement by estrogen. J Cell Biochem 2002;85:185–97.
[9] Zhao S, Zhang YK, Harris S, Ahuja SS, Bonewald LF. MLO-Y4 osteocyte-like cells support osteoclast formation and activation. J Bone Miner Res 2002;17:2068–79.
[10] Rubin J, Rubin C, Jacobs CR. Molecular pathways mediating mechanical signaling in bone. Gene 2006;367:1–16.
[11] Bonewald LF. Osteocytes as dynamic multifunctional cells. Ann N Y Acad Sci 2007;1116:281–90.
[12] Bakker AD, Silva VC, Krishnan R, Bacabac RG, Blaauboer ME, Lin YC, et al. Tumor necrosis factor alpha and interleukin-1beta modulate calcium and nitric oxide signaling in mechanically stimulated osteocytes. Arthritis Rheum 2009;60:3336–45.
[13] Kamioka H, Sugawara Y, Murshid SA, Ishihara Y, Honjo T, Takano-Yamamoto T. Fluid shear stress induces less calcium response in a single primary osteocyte than in a single osteoblast: implication of different focal adhesion formation. J Bone Miner Res 2006;21:1012–21.
[14] Jorgensen NR, Geist ST, Civitelli R, Steinberg TH. ATP- and gap junction-dependent intercellular calcium signaling in osteoblastic cells. J Cell Biol 1997;139:497–506.
[15] Guo XE, Takai E, Jiang X, Xu Q, Whitesides GM, Yardley JT, et al. Intracellular calcium waves in bone cell networks under single cell nanoindentation. Mol Cell Biomech 2006;3:95–107.
[16] Lu XL, Huo B, Chiang V, Guo XE. Osteocytic network is more responsive in calcium signaling than osteoblastic network under fluid flow. J Bone Miner Res 2012;27:563–74.
[17] Civitelli R, Beyer EC, Warlow PM, Robertson AJ, Geist ST, Steinberg TH. Connexin43 mediates direct intercellular communication in human osteoblastic cell networks. J Clin Invest 1993;91:1888–96.
[18] Adachi T, Aonuma Y, Taira K, Hojo M, Kamioka H. Asymmetric intercellular communication between bone cells: propagation of the calcium signaling. Biochem Biophys Res Commun 2009;389:495–500.
[19] Chen NX, Ryder KD, Pavalko FM, Turner CH, Burr DB, Qiu J, et al. Ca^{2+} regulates fluid shear-induced cytoskeletal reorganization and gene expression in osteoblasts. Am J Physiol Cell Physiol 2000;278:C989–97.
[20] Donahue SW, Jacobs CR, Donahue HJ. Flow-induced calcium oscillations in rat osteoblasts are age, loading frequency, and shear stress dependent. Am J Physiol Cell Physiol 2001;281:C1635–41.
[21] Bancroft GN, Sikavitsas VI, van den Dolder J, Sheffield TL, Ambrose CG, Jansen JA, et al. Fluid flow increases mineralized matrix deposition in 3D perfusion culture of marrow stromal osteoblasts in a dose-dependent manner. Proc Natl Acad Sci USA 2002;99:12600–5.
[22] Ishihara Y, Sugawara Y, Kamioka H, Kawanabe N, Kurosaka H, Naruse K, et al. In situ imaging of the autonomous intracellular Ca^{2+} oscillations of osteoblasts and osteocytes in bone. Bone 2012;50:842–52.
[23] Doty SB. Morphological evidence of gap junctions between bone cells. Calcif Tissue Int 1981;33:509–12.
[24] Yellowley CE, Li Z, Zhou Z, Jacobs CR, Donahue HJ. Functional gap junctions between osteocytic and osteoblastic cells. J Bone Miner Res 2000;15:209–17.
[25] Cotrina ML, Lin JH, Alves-Rodrigues A, Liu S, Li J, Azmi-Ghadimi H, et al. Connexins regulate calcium signaling by controlling ATP release. Proc Natl Acad Sci USA 1998;95:15735–40.
[26] Ziambaras K, Lecanda F, Steinberg TH, Civitelli R. Cyclic stretch enhances gap junctional communication between osteoblastic cells. J Bone Miner Res 1998;13.
[27] Donahue HJ. Gap junctions and biophysical regulation of bone cell differentiation. Bone 2000;26:417–22.
[28] Sanderson MJ, Charles AC, Boitano S, Dirksen ER. Mechanisms and function of intercellular calcium signaling. Mol Cell Endocrinol 1994;98:173–87.
[29] Cheng B, Zhao S, Luo J, Sprague E, Bonewald LF, Jiang JX. Expression of functional gap junctions and regulation by fluid flow in osteocyte-like MLO-Y4 cells. J Bone Miner Res 2001;16:249–59.
[30] Robinson JA, Chatterjee-Kishore M, Yaworsky PJ, Cullen DM, Zhao W, Li C, et al. Wnt/beta-catenin signaling is a normal physiological response to mechanical loading in bone. J Biol Chem 2006;281:31720–8.
[31] Kamioka H, Ishihara Y, Ris H, Murshid SA, Sugawara Y, Takano-Yamamoto T, et al. Primary cultures of chick osteocytes retain functional gap junctions between osteocytes and between osteocytes and osteoblasts. Microsc Microanal 2007;13:108–17.
[32] Ishihara Y, Kamioka H, Honjo T, Ueda H, Takano-Yamamoto T, Yamashiro T. Hormonal, pH, and calcium regulation of connexin 43-mediated dye transfer in osteocytes in chick calvaria. J Bone Miner Res 2008;23:350–60.
[33] Grimston SK, Brodt MD, Silva MJ, Civitelli R. Attenuated response to in vivo mechanical loading in mice with conditional osteoblast ablation of the connexin43 gene (Gja1). J Bone Miner Res 2008;23:879–86.
[34] Civitelli R. Cell–cell communication in the osteoblast/osteocyte lineage. Arch Biochem Biophys 2008;473:188–92.
[35] Lecanda F, Warlow PM, Sheikh S, Furlan F, Steinberg TH, Civitelli R. Connexin43 deficiency causes delayed ossification, craniofacial abnormalities, and osteoblast dysfunction. J Cell Biol 2000;151:931–43.
[36] Taylor AF, Saunders MM, Shingle DL, Cimbala JM, Zhou Z, Donahue HJ. Mechanically stimulated osteocytes regulate osteoblastic activity via gap junctions. Am J Physiol Cell Physiol 2007;292:C545–52.
[37] Lee DJ, Hsu YH. Fluid flow in capillary suction apparatus. Ind Eng Chem Res 1992;31:2379–85.
[38] Okada Y, Ueda S. Electrical membrane responses to secretagogues in parietal cells of the rat gastric mucosa in culture. J Physiol 1984;354:109–19.
[39] Joris L, Quinton PM. Filter paper equilibration as a novel technique for in vitro studies of the composition of airway surface fluid. Am J Physiol 1992;263:L243–8.
[40] Kamioka H, Honjo T, Takano-Yamamoto T. The three-dimensional distribution of osteocyte processes revealed by the combination of confocal laser scanning microscopy and differential interference contrast microscopy. Bone 2001;28:145–9.
[41] Wade MH, Trosko JE, Schindler M. A fluorescence photobleaching assay of gap junction-mediated communication between human cells. Science 1986;232:525–8.
[42] Ciani C, Doty SB, Fritton SP. An effective histological staining process to visualize bone interstitial fluid space using confocal microscopy. Bone 2009;44:1015–7.
[43] Adachi T, Aonuma Y, Tanaka M, Hojo M, Takano-Yamamoto T, Kamioka H. Calcium response in single osteocytes to locally applied mechanical stimulus: differences in cell process and cell body. J Biomech 2009;42:1989–95.
[44] Davidson JS, Baumgarten IM. Glycyrrhetinic acid derivatives: a novel class of inhibitors of gap-junctional intercellular communication. Structure–activity relationships. J Pharmacol Exp Ther 1988;246:1104–7.
[45] Hamill OP, McBride Jr DW. The pharmacology of mechanogated membrane ion channels. Pharmacol Rev 1996;48:231–52.
[46] Huo B, Lu XL, Costa KD, Xu Q, Guo XE. An ATP-dependent mechanism mediates intercellular calcium signaling in bone cell network under single cell nanoindentation. Cell Calcium 2010;47:234–41.
[47] Weinbaum S, Cowin SC, Zeng Y. A model for the excitation of osteocytes by mechanical loading-induced bone fluid shear stresses. J Biomech 1994;27:339–60.
[48] Piekarski K, Munro M. Transport mechanism operating between blood supply and osteocytes in long bones. Nature 1977;269:80–2.
[49] Lean JM, Mackay AG, Chow JW, Chambers TJ. Osteocytic expression of mRNA for c-fos and IGF-I: an immediate early gene response to an osteogenic stimulus. Am J Physiol 1996;270:E937–45.
[50] Peake MA, Cooling LM, Magnay JL, Thomas PB, El Haj AJ. Selected contribution: regulatory pathways involved in mechanical induction of c-fos gene expression in bone cells. J Appl Physiol 2000;89:2498–507.
[51] Resendez Jr E, Ting J, Kim KS, Wooden SK, Lee AS. Calcium ionophore A23187 as a regulator of gene expression in mammalian cells. J Cell Biol 1986;103:2145–52.
[52] Bravo R, Burckhardt J, Curran T, Müller R. Stimulation and inhibition of growth by EGF in different A431 cell clones is accompanied by the rapid induction of c-fos and c-myc proto-oncogenes. EMBO J 1985;4:1193–7.
[53] Moore JP, Todd JA, Hesketh TR, Metcalfe JC. c-fos and c-myc gene activation, ionic signals, and DNA synthesis in thymocytes. J Biol Chem 1986;261:8158–62.
[54] Schaefer A, Magócsi M, Fandrich A, Marquardt H. Stimulation of the Ca^{2+}-mediated egr-1 and c-fos expression in murine erythroleukaemia cells by cyclosporin A. Biochem J 1998;335:505–11.
[55] Burger EH, Klein-Nulend J. Mechanotransduction in bone—role of the lacuno-canalicular network. FASEB J 1999;13:S101–12.
[56] Price C, Zhou X, Li W, Wang L. Real-time measurement of solute transport within the lacunar–canalicular system of mechanically loaded bone: direct evidence for load-induced fluid flow. J Bone Miner Res 2011;26:277–85.
[57] Wang Y, McNamara LM, Schaffler MB, Weinbaum S. A model for the role of integrins in flow induced mechanotransduction in osteocytes. Proc Natl Acad Sci USA 2007;104:15941–6.
[58] Parekh AB. Decoding cytosolic Ca^{2+} oscillations. Trends Biochem Sci 2011;36:78–87.

[59] Sun S, Liu Y, Lipsky S, Cho M. Physical manipulation of calcium oscillations facilitates osteodifferentiation of human mesenchymal stem cells. FASEB J 2007;21:1472–80.
[60] You J, Reilly GC, Zhen X, Yellowley CE, Chen Q, Donahue HJ, et al. Osteopontin gene regulation by oscillatory fluid flow via intracellular calcium mobilization and activation of mitogen-activated protein kinase in MC3T3-E1 osteoblasts. J Biol Chem 2001;276:13365–71.
[61] Bennett MV, Contreras JE, Bukauskas FF, Sáez JC. New roles for astrocytes: gap junction hemichannels have something to communicate. Trends Neurosci 2003;26:610–7.
[62] Evans WH, De Vuyst E, Leybaert L. The gap junction cellular internet: connexin hemichannels enter the signalling limelight. Biochem J 2006;397:1–14.
[63] Schalper KA, Palacios-Prado N, Retamal MA, Shoji KF, Martínez AD, Sáez JC. Connexin hemichannel composition determines the FGF-1-induced membrane permeability and free [Ca2+]i responses. Mol Biol Cell 2008;19:3501–13.